Differential Responses of Cultured MC3T3-E1 Cells to Dynamic and Static Stimulated Effect of Microgravity in Cell Morphology, Cytoskeleton Structure and Ca^{2+} Signaling

Mingzhi Luo[1,2], Peili Yu[1], Yang Jin[3], Zhili Qian[1], Yue Wang[1], Jingjing Li[1], Peng Shang[2]*and Linhong Deng[1]*

Abstract: Random positioning machine (RPM) and diamagnetic levitation are two essential ground-based methods used to stimulate the effect of microgravity in space life science research. However, the force fields generated by these two methods are fundamentally different, as RPM generates a dynamic force field acting on the surface in contact with supporting substrate, whereas diamagnetic levitation generates a static force field acting on the whole body volume of the object (e.g. cell). Surprisingly, it is hardly studied whether these two fundamentally different force fields would cause different responses in mammalian cells. Thus we exposed cultured MC3T3-E1 osteoblasts to either dynamically stimulated effect of microgravity (d-μg) with RPM or statically stimulated effect of microgravity (s-μg) with diamagnetic levitation, respectively, for 3 h. Subsequently, the cells were examined for changes in cell morphology, cytoskeleton (CSK) structure and Ca^{2+} signaling. The results show that compared to the condition of normal gravity (1g), both d-μg and s-μg resulted in decrease of cell area and disruption of the microfilaments and microtubules in MC3T3-E1 cells, but cells under d-μg were more smooth and round while those under s-μg exhibited more protrusions. The decrease of cell area and disruption of microfilaments and microtubules induced by d-μg but not s-μg were rescued by inhibition of the stretch-activated channel by gadolinium chloride (Gd). Inhibition of calmodulin (CaM) by inhibitor, W-7, promoted the effects of s-μg on cell area and CSK filaments, but inhibition of calmodulin-dependent protein kinase (CaMK) by inhibitor, KN-93, weakened d-μg-induced effects on cell area and cytoskeleton. In addition, both d-μg and s-μg decreased the CaM expression and CaMKⅡ activity in MC3T3-E1 cells. Furthermore, s-μg resulted in decrease of the intracellular free Ca^{2+} concentration ($[Ca^{2+}]_i$) in MC3T3-E1 cells, which was reversed by disrupting microfilaments with cytochalas in B (CytB). Instead, d-μg induced increase of $[Ca^{2+}]_i$, which was inhibited by Gd. Taken together these data suggest that dynamic and static stimulated microgravity cause different responses in MC3T3-E1 cells. The dynamic force

[1]Changzhou Key Laboratory of Respiratory Medical Engineering, Institute of Biomedical Engineering and Health Sciences, No. 1 Gehu Road, Wujin District, Changzhou University, Changzhou 213164, P.R.China;

[2] Key Laboratory for Space Bioscience & Biotechnology, School of Life Sciences, Northwestern Polytechnical University, 127 Youyi XiluRoad, Xi'an 710072, P.R. China;

[3] Key Lab of Biorheological Science and Technology, Ministry of Education, College of Bioengineering, Chongqing University, Chongqing 404100, P.R. China.

*Corresponding Author: Deng, L. H. Email: dlh@cczu.edu.cn

field acts on stretch-activated channels to induce microfilaments disruption and Ca^{2+} influx in MC3T3-E1 cells whereas the static force field directly induces microfilament disruption, which in turn decreases the $[Ca^{2+}]_i$ in MC3T3-E1 cells. Such findings may have important implications to better understanding microgravity related cellular events and their applications.

Keywords: Osteoblasts, diamagnetic levitation, RPM, cytoskeleton, calcium signaling.

1   Introduction

Life on earth has evolved while being constantly exposed to the omnipresent long range force of gravity (g). Therefore, all the living organisms including human beings have well adapted to the field of gravity to maintain their normal form, structure and physiological function. However, when astronauts are sent into space for long-term spaceflight, the gravitational force exerted on them rapidly decreases to almost zero as they move far away from earth. And it has soon been learned that the loss of gravity at least causes apparent acute loss of bone density in the astronauts [Arfat, et al. (2014)]. Thus the potential effects of microgravity (μg) on human health as well as on other life forms cause great attention among researchers in the field of space life science [Zhang, et al. (2017)].

In order to explore the underlying mechanism and countermeasures to the adverse effects of microgravity on human physiology such as bone loss at the cell level, researchers can send cultured cells into space within a spaceship and then study the cells' response to microgravity during and/or after the space flight [Ulbrich, et al. (2014)]. However, this approach is very expensive and time-consuming, let alone the technological challenges. The alternative is to expose the cultured cells to stimulated the effect of microgravity on earth, which is to study the microgravity effect on cells by so-called ground-based method [Zhang, et al. (2016); Sambandam et al. (2016)]. There are two known ground-based methods for stimulation of microgravity. One is to levitate the cultured cells in a strong gradient magnetic field [Valles Jr, et al. (2005); Wang, et al. (2015)], and the other is to rotate the cultured cells in a random fashion by using a random positioning machine (RPM) [Zhang, et al. (2015); Borst and Van Loon (2008); Pani, et al. (2013)].

These two methods have been widely used to stimulate the effect of microgravity on cultured cells for investigation of corresponding cellular responses, without questioning the difference between them [Kopp, et al. (2016); Hu, Li, et al. (2015)]. In principle, however, these two methods generate fundamentally different force fields on cells. In a magnetic field with high strength and large gradient, usually produced by a superconducting magnet, a static levitation force will be generated in a diamagnetic object such as the cell, which counteracts the apparent gravity and thus provides the cell with an environment of stimulated effect of microgravity [Hammer, Kidder, Williams, et al. (2009)]. The diamagnetic levitation force can be strong enough to lift cells [Souza, et al. (2010)] and even a live frog [Berry and Geim (1997)]. By contrast, the typical RPM comprises two frames which are driven independently by two motors, resulting in a random orientation of the inner frame on which the cells are placed [Van Loon (2007)].

Thus, the continuous random change of orientation relative to the gravity vector dynamically results in a total zero net force experienced by the cells over a time period [Wuest, et al. (2015)].

Despite the obvious difference, few have examined whether cells respond differently to these two different kinds (i.e. dynamic versus static) of microgravity effect. Nevertheless, the previous studies using one way or the other to stimulate the effect of microgravity have discovered various important phenomena. For example, Hughes-Fulford and his colleagues have shown that osteoblasts can sense gravity change through mechanosensitive cytoskeleton (CSK) and ion channels, which may be responsible for bone remolding in astronauts during spaceflight [Hughes-Fulford (2003)]. Others have also confirmed the role of ion channels in gravity sensing of osteoblasts [Luo, et al. (2013)].

In 1999, Ingber proposed a hypothesis for the underlying mechanism of (micro)gravity sensing in animal cells based on mechanotransduction signaling pathways involving ion channels, CSK structures and protein kinase activation [Ingber (1999)]. In fact, under the condition of normal gravity, it has been shown that stretch-activated channels mediate a variety of essential functions such as proliferation and apoptosis in osteoblasts [Sun et al. (2014)], and these functions are most likely controlled by Ca^{2+}, calmodulin (CaM), and CaM dependent protein kinase Ⅱ (CaMKⅡ) signaling pathway [Sanabria, Swulius, Kolodziej, et al. (2009)] and CSK organization including act in filaments and microtubules.

According to our knowledge, so far there is only one previous study that compared in parallel the cell's response to both diamagnetic levitation and RPM rotation. It is reported that the two ground-based methods caused changes of the microfilaments in cultured A431 cells, similar as those observed in A431 cells when exposed to real microgravity in space [Moes MJA, et al.(2011)]. However, in the above study, A431 cells are a cell line derived from human epidermal carcinoma that is not involved in bone formation and remodeling. Furthermore, the comparative results are only qualitative, which may not reveal subtle differences between the test samples. Therefore, the principles and force fields of the RPM and diamagnetic levitation conditions are different. The gravity under the RPM rotation and magnetic levitation is always acting on the sample, but its direction is either dynamically changing at any given instant in RPM or constantly static in the magnetic levitation when the samples are compared, respectively. Additionally, under the RPM condition, cells as soft matters are rotated and massaged by the gravity, and the cytoplasm and large organelle in cells may change their locations resulting in the alterations of stress in cells and the tension in cell membranes. But in the diamagnetic levitation, the force of gravity is constant and compensated on the level of individual molecule by tiny magnetized forces, so CSK system supporting the cell may change their structure. Therefore, we hypothesized that cells may respond to the dynamic and static stimulated μg differently.

Osteoblasts can sense the change of force including gravity and regulate the bone remodeling. Many hypotheses about the gravity sensing system in animal cells have been proposed [Zhang, et al. (2017); Ingber (1999)]. The possible regulatory sensors which are sensitive to microgravity include mechanosensitive ion channels and CSK [Hughes-Fulford

(2003)]. Ion channels can sense the change of gravity [Luo, et al.(2013), Gillespie and Walker (2001)]. Stretch-activated channels mediate a variety of functions in osteoblasts. Ca^{2+}, CaM, and CaMKⅡ signaling pathway controls a variety of essential cellular behaviors such as proliferation, apoptosis and CSK organization [Sanabria, Swulius, Kolodziej, et al. (2009)].

In this study, we investigated the responses of MC3T3-E1 cells, a mouse osteoblast cell line, to magnetic levitation (static stimulated effect of microgravity, s-μg), or RPM rotation (dynamic stimulated microgravity, d-μg), respectively, by quantitative evaluation and comparison of the cell morphology, CSK and Ca^{2+} signaling. Consequently, we found that MC3T3-E1 cells responded differently to static and dynamic stimulated effect of microgravity. Such differences suggest that the current ground-based methods may be all limited by their own feature in revelation of the true work of microgravity on living cells, and space still remains the non-substitutable place to conduct ultimate tests for such inquiry.

2   Materials and methods

2.1 Chemicals and reagents

Cytochalasin B (CyoB, 857777), Gadolinium chloride (Gd, 203289), W-7 (A3281), KN-93 (K1385), Fluo-3/AM (F6142), anti-CaM (C7055), and anti-GAPDH (G8795) antibodies were purchased from Sigma-Aldrich (St. Louis, MO, USA). Rhodamine-labeled phalloidin was purchased from Thermo Fisher (R415). Anti-tubulin (556321) antibodies were purchased from BD Pharmingen (San Jose, CA, USA). Anti-CaMK (sc-13141) and anti-phosphoralated CaMK (sc-12886) antibodies were purchased from Santa Cruz (Dallas, TX, USA). Infrared (IR) labeled antibodies (goat-anti rabbit (925-32211) or goat-anti mouse (925-32210) were obtained from LI-COR (Lincoln, NE, USA). All other chemicals used were of the highest purity available.

2.2 Cell culture and drug experiments

MC3T3-E1 cells, a mouse osteoblastic cell line derived from calvarial cells, were obtained originally from American Type Culture Collection (ATCC, Manassas, VA, USA). Cells were cultured in alpha-minimal essential medium (α-MEM, SH30265.01, Hyclone, Logan, UT, USA) containing 10% fetal bovine serum (FBS,SH30070.03HI, Hyclone, Logan, UT, USA) and 100 U/ml penicillin and maintained in an environment of humidified air containing 5% CO_2 at 37 ℃. To block stretch-activated channels of the MC3T3-E1 cells, the cells were treated with Gd (100 nM) in culture for 30 min, and then, in the presence of Gd (100 nM) the cells were subjected to RPM or diamagnetic levitation conditions. Similarly, the cells were treated with either 10 μM W-7 (a CaM inhibitor), 2 μM KN-93 (a CaMK inhibitor), or 5 μM CytB (an actin-disrupting agent), respectively, in order to alter the cytoskeleton (CSK) structure and function during the *g* experiment.

2.3 Cell culture under dynamic stimulated microgravity

To dynamically stimulate the effect of microgravity (d-μg) on cultured cells, a random positioning machine (RPM) was used as described by van Loon [Van Loon (2007)]. The

RPM was manufactured by the Center for Space Science and Applied Research of the Chinese Academy of Sciences in Beijing [Borst and Van Loon (2008); Xiang, Qi , Dai, et al. (2010)]. The RPM is composed of an inner and an outer frame, and the rotation of each frame is random, autonomous, and controlled by a computer program.
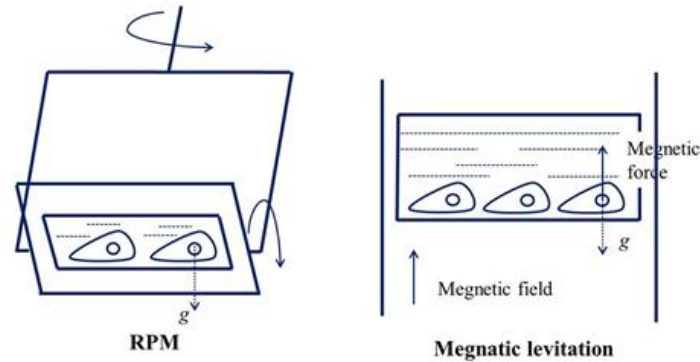
Figure 1: The different force field sensed by cells under the RPM and magnetic levitation system.

The gravity under the RPM rotation (left) and magnetic levitation (right) is always acting on the sample, but the direction is either dynamic in the RPM or static in the magnetic levitation when the samples are compared, respectively.

During d-mu$g$ experiment, MC3T3-E1 cells in standard culture dish were first detached by trypsin, and inoculated at a density of 2×10^4 cells/cm^2 onto glass coverslip (Greiner Bio-One, Frickenhausen, Germany) that was placed at the bottom of another cell culture dish. The cells were then allowed to well attach to the coverslip while maintained in an incubator at 37 ℃ and humidified atmosphere of 5% CO_2 for 24 h. Subsequently, the coverslip was inserted into a specially designed culture chamber, which was filled with MEM and 10% FBS (Fig. 1 left, air bubbles avoided). Each chamber accommodated three coverslips and tightly capped. A stack of three these chambers were placed on the inner frame of the RPM. Afterwards, the RPM machine was placed in an incubator at 37 ℃ and operated continuously for 3 h in a random rotation mode at the speed of 0.1~10 rpm for both the inner and outer frames of the chamber (16). The time-averaged gravitational vector acting on the cells in these chambersat the center of the frame was thus reduced to ~$2 \times 10^{-3}g$. Cells prepared in the same manner and placed under the same conditions, but not subjected to RPM were used as static control groups.

2.4 Cell culture under static stimulated microgravity

To statically stimulate the effect of microgravity (s-μg) on cultured cells, we used a superconducting magnet to establish a large gradient high magnetic field within which the cultured cells experienced a magnetic levitation (maglev) effect [Qian, et al. (2009); Glade, Beaugnon and Tabony (2006)]. The superconducting magnet (JMTA-16T50MF) was tailor-made by Japan Superconductor Technology Inc (JASTEC) according to our

design and specifications. Inside the bore of this superconducting magnet, the magnetization force (*f*) imposed on a specific diamagnetic material (e.g. cells) is determined as follows.

$$f = m\chi_\rho B \cdot (\frac{dB}{dz})$$
(1)

where χ_ρ stands for the specific magnetic susceptibility of the material, and both magnitude and direction of *f* vary as a function of the position (z) inside the bore. Therefore, according to our design specifications, we can generate an apparent gravity on the cultured cells ranging from near zero g to 2g by placing the cells at different positions inside the bore of the magnet. For comparison with d- g experiment, the cells were thus placed at the position where the apparent gravity was either near zero (s-μg) or 1g (as control groups), respectively.

During s-g experiment, MC3T3-E1 cells were prepared and treated in the same way as described in d- g experiment, but placed inside the bore of the superconducting magnet at the given positions. The temperature within the bore was kept at constant 37 ℃ by using the in-house built temperature control system and software.

2.5 Hematoxylin and eosin (HE) staining for morphological evaluation of the cultured cells

To evaluate the morphological changes of cultured MC3T3-E1 cells in response to stimulated microgravity, the cells were stained with hematoxylin and eosin (HE) and then examined using optical microscopy. In brief, MC3T3-E1 cells grown on glass coverslips were washed twice with 0.1 M phosphate buffered solution (PBS, pH 7.4) and fixed in 4% paraformaldehyde for 20 min. The cells were then incubated in 0.5% haematoxylin and 0.5% eosin for 10 and 5 min, respectively. Then the cells were dehydrated through an ascending gradient of ethanol, and were made transparent with dimethylbenzene. Digital images of the stained cells were acquired using a Nikon Eclipse 80i microscope (Nikon, Japan, 20 × objective). For each experimental group, one hundred cells were randomly selected and the coverage cell area (A) per cell was quantified using Image-Pro Plus 6.0 software. The ratio of A change induced by μg was calculated according to the equation: $R_A = (A^{\mu g} - A^{1g}) / A^{1g} \times 100\%$, in which $A^{\mu g}$ is the coverage cell area of MC3T3-E cells at d-μg or s-μg and A^{1g} is the coverage cell area of MC3T3-E cells at 1 g.

2.6 Fluorescence confocal microscopy for CSK evaluation of the cultured cells

To evaluate the CSK changes of cultured MC3T3-E1 cells in response to stimulated microgravity, the cells were stained with fluorescent dyes to label cytoskeletal components and then examined using laser scanning confocal microscopy. Briefly, MC3T3-E1 cells grown on glass coverslips were incubated with 500 μl4% paraformaldehyde in PBS for 10 min and permeabilized with 0.3% Triton X-100 detergent dissolved in PBS for 15 min. Then the cells were blocked with bovine serum

albumin (BSA, 1%) for 60 min at room temperature. Subsequently, the cells were incubated with mouse anti-α-tubulin (1: 20) at 4 ℃ overnight in a humid chamber. Afterwards, the cells were further incubated with rhodamine-labeled phalloidin and goat anti-mouse FITC-IgG in PBS solution supplemented with 1% BSA at room temperature for 60 min. Finally, the cells were observed and imaged by using a laser confocal scanning microscope (Leica SP5, Germany, 63 × objective) with an excitation wavelength at 496 nm and an emission wavelength at 516 nm.

2.7 Analysis of CSK structure of the cultured cells

The fluorescence microscopic images of the cultured cells, captured as described above, were further evaluated for quantitative distribution of the CSK microfilaments and microtubules. Briefly, each single cell captured on the microscopic images was separated and stored in a 200 ×200-pixel image. These single cell images were then converted to binary images (black and white), and then analyzed with the fractal box count to obtain the fractal dimension (D) of microfilaments or microtubules in a single cell by using ImageJ software (http://rsb.info.-nih.gov/ij) [Fuseler, Millette, Davis, et al. (2007)]. For each experimental group, more than 30 cells were analyzed and the averaged D value was used for following quantitative comparison. The ratio of D value change induced by μg was calculated according to the equation: $R_D = (D^{\mu g} - D^{1g}) / D^{1g} \times 100\%$, in which $D^{\mu g}$ is the D value of MC3T3-E cells at d-μg or s-μg and D^{1g} is the D value of MC3T3-E cells at 1 g.

2.8 Evaluation of CSK and contractile proteins of the cultured cells

Western blot analysis was employed to evaluate the expression of CSK and/or contractile proteins in MC3T3-E1 cells in response to stimulated microgravity conditions. In brief, MC3T3-E1 cells were lysed in ice-cold RIPA buffer (50 mM Tris-HCl, pH 8.0, 150 mM sodium chloride, 1% Nonidet P-40, 0.5% deoxycholate and 0.1% SDS) supplemented with protease inhibitors and 1 mM sodium orthovanadate for 30 min at 4 ℃, followed by centrifugation at 12,000 × g for 10 min at 4 ℃. Protein content of supernatant was examined by the Bio-Rad DC protein assay (Bio-Rad, Shanghai, China). Whole cell protein extracts (40 μg/lane) were separated by SDS-PAGE and transferred to a polyvinylidene difluoride (PVDF) membrane (Millipore Co., USA) using a Bio-Rad wet transfer system (Bio-Rad). Protein transfer efficiency and size determination were verified using pre-stained protein markers (Bio-Rad). Membranes were blocked with 5% non-fat milk in PBS for 1 h at room temperature, followed by overnight incubation at 4 ℃ with primary antibodies directed against GAPDH, CaM, CaMKⅡ, and pCaMKⅡ. Primary antibody binding was detected using an infrared-labeled secondary antibody and visualized by the ODYSSEY Infrared Imaging System (LI-COR, USA). Band intensity was quantified by using ImageJ software, and normalized to the corresponding GAPDH value. The ratio of protein expression change induced by μg was calculated according to the equation: $R_P = (P^{\mu g} - P^{1g}) / P^{1g} \times 100\%$, in which $P^{\mu g}$ is protein relative expression in MC3T3-E cells at d-μg or s-μg and P^{1g} is protein relative expression in MC3T3-E cells at 1 g.

2.9 Fluorecence confocal microscopy for evaluation of intracellular calcium signaling of the cultured cells

To evaluate the intracellular calcium signaling ($[Ca^{2+}]_i$) of the cultured MC3T3-E1 cells in response to stimulated microgravity, the cells were labeled with a calcium ion specific fluorescent dye (Fluo-3/AM) and then evaluated for the intensity of intracellular calcium signaling by using a laser confocal scanning microscope [Kao, Harootunian and Tsien (1989)]. Briefly, MC3T3-E1 cells grown on glass coverslips were first loaded with Fluo-3/AM (10 μM) dissolved in MEM at 37 ℃ in the dark for 30 min. Afterwards, the cells in culture were either or not exposed to stimulated microgravity. Subsequently, the cells were examined and imaged by using a laser confocal scanning microscope (Leica SP5, Germany, 63 ×objective), with fluorescence excitation and emission at 488 nm and 530 nm, respectively. For each experimental group, thirty cells were randomly selected and the fluorescence intensity per cell was digitized using the Leica Image Manager Software. $[Ca^{2+}]_i$ was calibrated according to the equation: $[Ca^{2+}]_i = K_d \times [F_{(t)} - F_{min}]/[F_{max} - F_{(t)}]$, in which $F_{(t)}$ is the measured fluorescence intensity of cells in each group and K_d is the Ca^{2+}-Fluo-3 dissociation constant (390 nM). The fluorescence values of maximum (F_{max}) and minimum (F_{min}) were obtained by adding 0.1% Triton X-100 (plus 5 mM $CaCl_2$) and 20 mM EGTA sequentially at the end of an experiment, respectively. The ratio of $[Ca^{2+}]_i$ change induced by $μg$ was calculated according to the equation: $R_{[Ca^{2+}]_i} = ([Ca^{2+}]_i^{μg} - [Ca^{2+}]_i^{1g}) / [Ca^{2+}]_i^{1g} \times 100\%$, in which $[Ca^{2+}]_i^{μg}$ is $[Ca^{2+}]_i$ in MC3T3-E cells at d-μg or s-μg and $[Ca^{2+}]_i^{1g}$ is $[Ca^{2+}]_i$ in MC3T3-E cells at 1 g.

2.10 Statisticalanalysis

Data are presented as mean ± standard deviation (SD). The significance of differences between the control and experimental groups was evaluated by Student's *t* test using GraphPad Prism 5 software version 5.0 for Windows (GraphPad Software Inc., USA). Differences were considered significant at $p < 0.05$.

3   Results

3.1 Morphological changes of EC3T3-E1 cells in response to dynamic or static μg

Fig. 2 shows the effects of dynamic and static stimulated microgravity (d-μg, s-μg, respectively) on the morphology of EC3T3-E1 cells. Under normal gravity (1g) for 3 h, MC3T3-E1 cells appeared to be well attached to the substrate and maintained in normal fibroblast-like shape (Fig. 2A-a,d). Compared to the cells at 1g as control, the EC3T3-E1 cells exposed to both d-μg and s-μg appeared to be largely reduced in cell size (Fig. 2A-b,c). However, the cells exposed to d-μg were more rounded up whereas those exposed to s-μg became more protruded in shape (Fig. 2A-b *vs.* Fig. 2A-c). The quantified results show that d-μg reduced the cell size (A) from 1563 ± 207 μm^2 (1g) to 1221 ± 201 μm^2 (d-μg) ($p < 0.01$, Fig. 2B-a left), and s-μg reduced the cell size from 1651 ± 195 μm^2 (1g) to 1123 ± 232 μm^2 (s-μg) ($p < 0.01$, Fig. 2B-a right), respectively. These data indicate that both d-μg and s-μg inhibited cell spreading, but d-μg was less potent

than s-μgin inhibiting cell spreading, as the former reduced the cell size by only 22% but the latter reduced the cell size by 32% ($p < 0.01$, Fig. 2C).

When the cells were exposed to *μg* in the presence of W-7, a CaM inhibitor, and KN-93, a CaMK II inhibitor, respectively, the effect of μg on cell spreading was altered, as shown in Fig. 2A-e to Fig. 2A-l. It appeared that W-7 impaired the cell spreading in all cases, but its effect was much greater on cells exposed to *μg*, esp. d-μg (Fig. 2A-f *vs.* Fig. 2A-e; Fig. 2A-g *vs.* Fig. 2A-h). Interestingly, in the presence of W-7 the cells exposed to d-μg became more protruded than those to s-μg (Fig. 2A-f *vs.* Fig. 2A-g). Quantitatively, the inhibition of CaM by W-7 reduced the cell size to $1201 \pm 124 \mu m^2$ for cells exposed to *1 g*, and further reduced the cell size to $1002 \pm 165\ \mu m^2$ for cells exposed to d-μg (Fig. 2B-b left, $p < 0.01$). For s-μg, W-7 reduced the cell size to $1424 \pm 138\ \mu m^2$ for cells exposed to *1 g*, and further reduced the cell size to$812 \pm 175\ \mu m^2$ for cells exposed to s-μg(Fig. 2B-b right, $p < 0.01$). However, as regards the effect of W-7 on cells exposed to either d-μg or s-μg, W-7 reduced the cell size by 17% for cells exposed to d-μg, but 43% for cells exposed to s-μg, as compared to their counterparts exposed to 1-μg, respectively ($p < 0.01$, Fig. 2C-b).
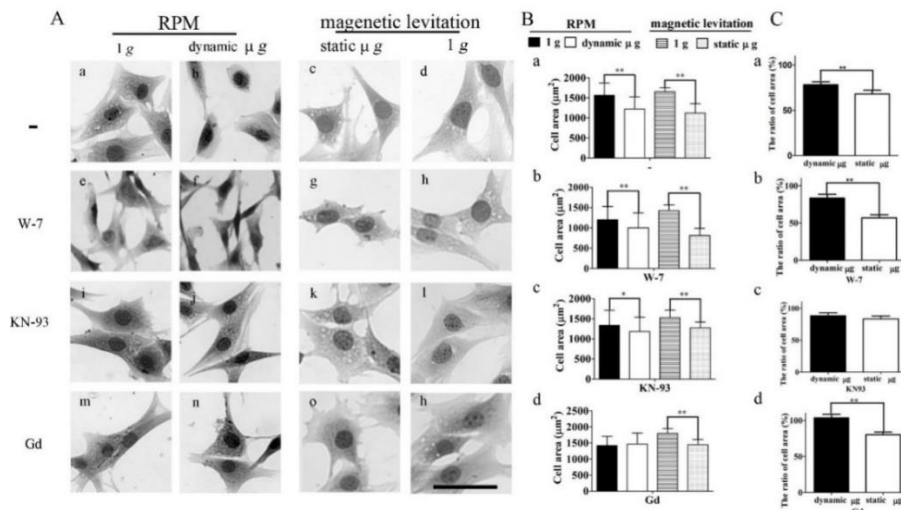
Figure 2: Changes in morphology and coverage area of MC3T3-E1 cells exposed to the dynamic and static μg.
A) Changes in cell morphology of MC3T3-E1 cells exposed to the dynamic and static μg were measured by HE staining method. Cells without drugs (a, b, c, d) or treated withW-7 (Gd, 20 μM, e, f, g, h), KN-93 (2 μM, i, j, k, l) and gadolinium chloride (Gd, 100 nM, m, n, o, p) were cultured under the 1g and different stimulated μg (dynamic and static) conditions for 3 h. Photographs were taken with a light microscope. Scale bar represents 100 μm. B) Histogram shows changes in cell size of MC3T3-E1 cells exposed to dynamic and static μg. For each group, single cell (n = 100) was randomly selected and cell area was quantified with Image-Pro plus 6.0 software. C) Histogram shows the ratio of cell area change of MC3T3-E1 cells exposed to dynamic and static μg. Values are shown as the mean ± SD. Statistically significant differences are indicated as $^*p < 0.05$,

[**]*p*< 0.01.

Although KN-93 seemed not to affect the cell shape dramatically (Fig. 2A-i to Fig. 2A-a) and also generally reduced the cell size in all cases (1339 ± 172 μm^2 vs. 1183 ± 156 μm^2 for1g *vs.*d-μg, and 1528 ± 187 μm^2*vs.* 1273 ± 141 μm^2 for 1g and s-μg, respectively, in the presence of KN-93, *p*< 0.05, Fig. 2B-c), it appeared to diminish the different cell spreading in response to d-μgor s-μg as the ratio of cell area reduction due to d-μg or s-μg in the presence of KN-93 was indifferent (12% *vs.* 17%, NS, Fig. 2C-c).

Interestingly, when exposed to μg in the presence of Gd, an inhibitor of the stretch-activated channels, the cells under d-μg displayed fibroblast-like shape, but the cells under s-*μg* appeared to be with more protrusions (Fig. 2A-m to 2A-p). And the cell size did not change much in response to d-μg (1411 ± 193 μm^2*vs.*1462 ± 242 μm^2 for 1*gvs.* d-μg, NS, Fig. 2B-d/left), but reduced from 1798 ± 146 μm^2 to 1441 ± 162 μm^2 in response to s-μg (1*gvs.* s-μg, *p*<0.05, Fig. 2B-d right). Therefore, the ratio of cell area changes due to d-μg or s-μg in the presence of Gd was still significantly different (4% *vs.* -20%, Fig. 2C-d).

3.2 CSK reorganization of EC3T3-E1 cells in response to dynamic and static *μg*

Fig. 3 shows the effects of d-μg and s-*μg* on the microfilaments of MC3T3-E1 cells. Under normal gravity (1g) for 3h, MC3T3-E1 cells appeared to have abundant stress fibers (Fig. 3A-a,d). Compared to the cells at 1 gas control, MC3T3-E1 cells exposed to both d-μg and s-μg show disrupted microfilaments, and the faint microfilaments mostly arranged in the peripheral region and few stress fibers in the central region of the cell (Fig. 3A-b,c). The quantified results show that d-μg and s-μg caused the cells to reduce the fractal dimension of microfilaments (D$_{MF}$) from 1.74 ± 0.09 (1g) to 1.62 ± 0.03 (d-μg) (*p*< 0.01, Fig. 3B-a left), and from 1.75 ± 0.04 (1g) to 1.56 ± 0.03 (s-μg) (*p*< 0.01, Fig. 3B-a right), respectively. These data show that both d-μg and s-μg significantly decreased D$_{MF}$, but d-μg was less potent than s-μg in disrupting the microfilament, as the former decrease D$_{MF}$ by only 7% but the latter decreased D$_{MF}$ by 11% (p<0.05, Fig. 3C-a).
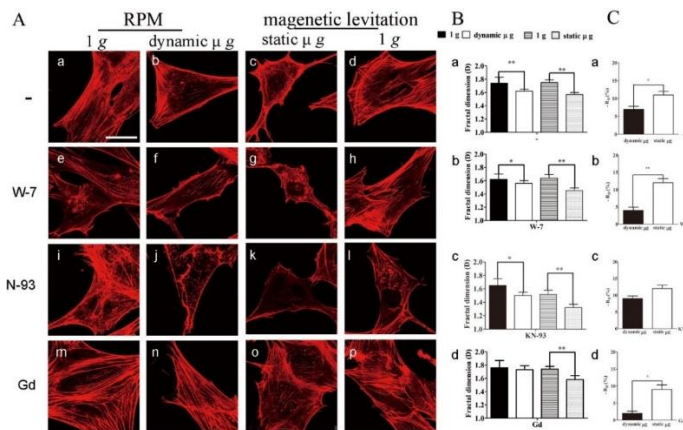
Figure 3: Laser scanning confocal microscopy analysis of the effects of the dynamic and static *μg* on microfilaments in MC3T3-E1.
A) Cells without drugs (a, b and c, d) or treated with W-7 (Gd, 20 μM, e, f and g, h),

KN-93 (2 μM, i, j and k, l), and gadolinium chloride (Gd, 100 nM, m, n and o, p) were cultured under the1g(control), dynamic or static *μg* conditions for 3 h, and microfilaments (MF) were probed with rhodamine-labeled phalloidin and FITC-labeled anti-tubulin antibody. The images of cytoskeleton in MC3T3-E1 cells were visualized with a laser confocal scanning microscope. Scale bar represents 25 μm. B) Histograms show changes in microfilament dimension of MC3T3-E1 cells under the dynamic and static μg. For each group, single cell (n = 30) was randomly selected and fractal dimension was quantified with ImageJ software. C) Histogram shows changes in the ratio of fractal dimension of microfilaments in MC3T3-E1 cells exposed to dynamic and static μg. Values are shown as the mean ± SD. Statistically significant differences are indicated as $^*p < 0.05$, $^{**}p < 0.01$.

When the cells were exposed to *μg* in the presence of W-7, a CaM inhibitor, and KN-93, a CaMK inhibitor, respectively, the effect of *μg* on the distribution of microfilament was altered, as shown in Fig. 3A-e to Fig.3A-i. It appeared that W-7 disrupted the microfilaments in all cases, but its effect was much greater on cells exposed to μg, esp.s-μg (Fig. 3A-f *vs.* Fig. 3A-e; Fig. 3A-g *vs.* Fig. 3A-h). Quantitatively, in the presence of W-7, D_{MF} decreased to 1.62 ± 0.08 and 1.64 ± 0.05 when cells exposed to 1g, and further decreased to 1.56 ± 0.04 and 1.45 ± 0.04 when cells exposed to d-μg ($p < 0.01$, Fig. 3B-b left) or s-μg($p < 0.01$, Fig. 3B-b right), respectively. However, as regards the effect of W-7 on cells exposed to either d-μg or s-μg, W-7 reduced D_{MF} by 4% for cells exposed to d-μg, but 12% for those exposed to s-μg, as compared to exposed to 1g, respectively ($p < 0.01$, Fig. 3C-b).

KN-93 also disrupted the microfilaments in all cases, but its effect was much greater on cells exposed to s-μg (Fig. 3A-j *vs.* Fig. 3A-i; Fig. 3A-k *vs.* Fig. 3A-l). Quantitatively, disruption of CaMK by KN-93 decreased D_{MF} to 1.65 ± 0.10 for cells exposed to 1g, and further reduced it to 1.50 ± 0.05 for cells exposed to d-μg ($p < 0.01$, Fig. 3B-c left). In contrast, KN-93 reduced D_{MF} from 1.52 ± 0.05 to 1.34 ± 0.04 when the exposure was changed from 1g to s-μg($p < 0.01$, Fig. 3B-c right). However, as regards the effect of KN-93 on cells exposed to either d-μg or s-μg, it appeared that there was no difference in the extent of KN-93 induced microfilament disruption (-9% *vs.* -12%, NS, Fig. 3C-c).

Interestingly, in the presence of Gd, an inhibitor of the stretch-activated channels, the cells exposed to d-μg still show marked stress fibers, however, those exposed to s-μg show few stress fibers (Fig. 3-m to Fig. 3-p). The quantified D_{MF} was not affected in response to d-μg (1.76 ± 0.11 *vs.* 1.73 ± 0.06 for 1g*vs.*d-μg, NS, Fig. 3B-d left)*,* but decreased in response tos-μg (1.74 ± 0.04 *vs.* 1.58 ± 0.06 for 1g *vs.* s-μg,$p < 0.01$, Fig. 3B-d right). Therefore, Gd induced less extent of microfilament disruption in cells exposed to d-μg than in those exposed to s-μg (-2% *vs.* -9%, $p < 0.05$, Fig. 3C-d).

Fig. 4 shows the effects of d-μg and s-μg on the microtubules of MC3T3-E1 cells. When exposed to 1g, the cells appeared to have microtubule filaments radiating from the microtubule organizing center and branched toward the cell membrane (Fig. 4A-a,d). In contrast, when exposed to either d-μg or s-μg, the cells appeared to have disturbed microtubules (Fig. 4 A-b, c). The quantified fractal dimension value of microtubules (D_{MT}) for cells exposed to d-μg decreased to 1.55 ± 0.03 from 1.61 ± 0.06 at 1g ($p < 0.01$, Fig. 4-a left), and for cells exposed to s-μg decreased to 1.47 ± 0.06 from 1.63 ± 0.07 at

1g ($p< 0.01$, Fig. 4B-a right), respectively. These data indicate that both d-μg and s-*μg* induced significant disruption of microtubules in the cells. However, d-μg was less potent than s-μg for microtubule disruption, as the former decreased D_{MT} by only 4% but the latter by 10% ($p< 0.05$, Fig. 4C-a).
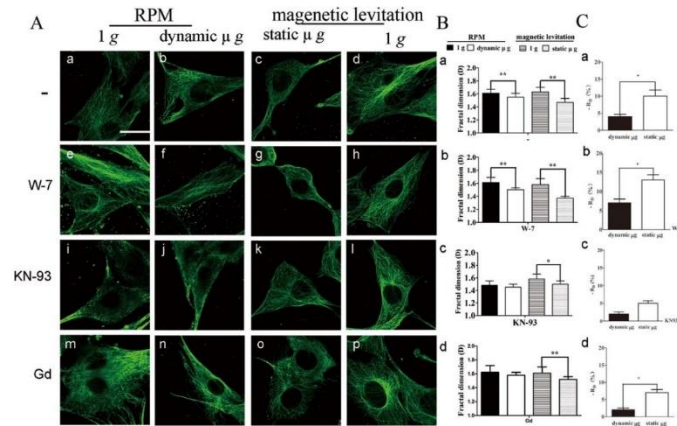
Figure 4: Laser scanning confocal microscopy analysis of the effects of the dynamic and static *μg* on microtubules in MC3T3-E1.

A) Cells without drugs (a, b and c, d) or treated with W-7 (Gd, 20 μM, e, f and g, h), KN-93 (2 μM, i, j and k, l), and gadolinium chloride (Gd, 100 nM, m, n and o, p) were cultured under 1g (control), dynamic or static stimulated μg conditions for 3 h, and microtubules were probed with FITC-labeled anti-tubulin antibody. Photographs were taken with a laser confocal scanning microscope. Scale bar represents 25 μm. B) Histogram shows changes in microtubule fractal dimension of MC3T3-E1 cells exposed to 1g *vs.* dynamic μg or 1g*vs.* static μg. For each group, single cell (n = 30) was randomly selected and fractal dimension was quantified with ImageJ software. C) Histogram shows the ratio of fractal dimension change of microtubules in MC3T3-E1 cells exposed to dynamic and static *μg*. Values are shown as the mean ± SD. Statistically significant differences are indicated as [*]$p< 0.05$, [**]$p< 0.01$

In the presence of W-7, the effect of *μg* on microtubule structure was altered as shown in Fig. 4A-e to Fig. 4A-i. It appeared that W-7 disrupted the microtubule structure in all cases, but the effect was most evident in cells exposed to s-μg (Fig. 4A-f *vs.* Fig. 4A-e; Fig. 4A-g *vs.* Fig. 4A-h). Quantitatively, W-7 caused D_{MT} to decrease to 1.61 ±0.06 for cells exposed to 1g, and further decrease to1.50 ±0.04 for cells exposed to d-μg (Fig. 4B-b left), and for cells exposed to s-μg decreased to 1.37 ±0.06 from 1.58 ±0.07 at 1g(Fig. 4B-b right), respectively. As regards the effect of W-7 on cells exposed to either d-μg or s-μg, W-7 induced D_{MT} reduction by 7% in cells exposed to d-μg, but 13% in those exposed to s-μg, as compared to respective corresponding values at 1g (Fig. 4C-b).

KN-93 also disrupted the structure of microtubules in all cases, but much more so for cells exposed to d-μg (Fig. 4A-j *vs.* Fig. 4A-i; Fig. 4A-k *vs.* Fig. 4A-l). Quantitatively, for cells exposed to d-μg,KN-93 reduced D_{MT} from baseline (1.61 ±0.06) to 1.48 ±0.07 at 1g, and 1.45 ±0.05 at d-μg, respectively (Fig. 4B-c left). For cells exposed to s-μg,

KN-93 reduced D_{MT} from baseline (1.63 ± 0.07) to 1.58 ± 0.08 at 1g, and 1.50 ± 0.05 at s-μg(Fig. 4B-c right). However, as regards the effect of KN-93 on cells exposed to either d-μg or s-μg, there was no difference in the extent of KN-93 induced microtubule disruption (Fig. 4C-c).

Similar as for microfilaments, Gd caused greater disruption of the microtubule bundles in cells exposed to s-μgas compared to in those exposed to d-μg (Fig. 4-m to Fig. 4-p). Quantitatively, Gd caused D_{MT} to decrease from 1.62 ± 0.10at 1g to 1.58 ± 0.04 at d- g (4B-d left), but decrease from 1.63 ± 0.04 at 1g to 1.52 ± 0.06 ats-μg. The extents of Gd-induced decrease in D_{MT} in cells exposed to d-μg and s-μg were significantly different (2% *vs.* 7%, *p*< 0.05, Fig. 4C-d).

3.3 Dynamic and static μg inhibited CaM/CaMK signaling

Fig. 5 shows the effect of d-μg and s-μg on CaM expression and CaMKⅡ activity in MC3TC-E1 cells. When exposed to d-μg, the expression of CaM in the cells decreased from that at 1g as shown by the Western blot results (Fig. 5A upper). The quantified results show that the relative expression of CaMs decreased from 0.35 ± 0.03 at 1g to 0.24 ± 0.04 at d-μg ($p < 0.01$, Fig. 5B-a), and from 0.19 ± 0.01 at 1g to 0.15 ± 0.03 at s-μg ($p < 0.01$, Fig. 5B-a), respectively. These data indicate that both d-μg and s-μg significantly decreased the CaM expression, but s-μg was less potent than d-μg in doing so, as the former decreased the D value by only 21% but the latter decreased the D value by 31% (*p*< 0.01, Fig. 5C-a).

The Western blot results show that the CaMKⅡ activity in MC3T3-E1 cells exposed to d-μg decreased when compared at 1g (Fig. 5A bottom). The relative CaMKⅡ activity decreased from 0.25 ± 0.01 at 1g to 0.15 ± 0.01 at d-μg (*p*< 0.01, Fig. 5B-a), and from 0.33 ± 0.05 at 1g to 0.22 ± 0.04 at s-μg(*p*< 0.01, Fig. 5B-b), respectively. These data indicate that d-μg and s-μg both significantly decreased the CaMKⅡ activity, but s-μg was less potent than d-μg in doing so, as the former decrease the D value by only 33% but the latter decreased the D value by 40% (*p*<0.05, Fig. 5C-b).
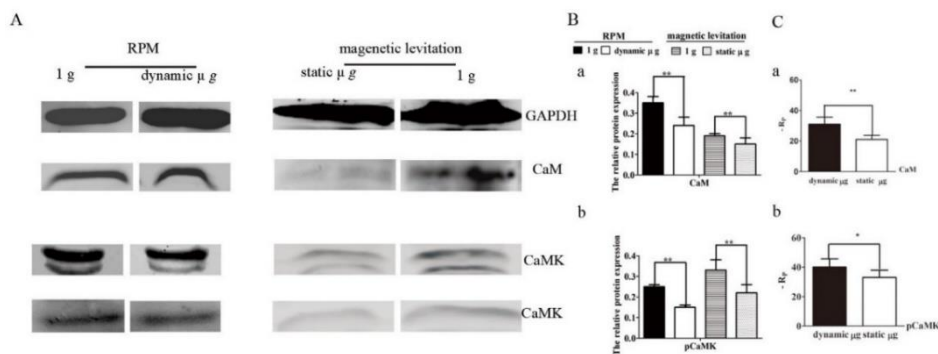
Figure 5: Western blot analysis of the CaM expression and CaMKⅡ activity in MC3T3-E1 cells under d-μg and s-μg.

A) After 3 h exposure to the d-μg and s-μg, cells were lysed and the whole cell lysates (40 μg each) were immunoblotted with specific antibodies against GAPDH, caM,

CaMKⅡ, and p-CaMKⅡ. B) Relative densitometric analysis of the bands was performed by ImageJ. Histograms are shown as the mean ± SD from triplicate samples for the CaM expression and the active CaMKⅡ expression. C) Histogram shows the ratio of protein expression change of CaM and p-CaMKⅡ in MC3T3-E1 cells exposed to d-μg and s-μg. Statistically significant differences are indicated as [**]$p < 0.01$.

3.5 The calcium concentration changes induced by the dynamic and static μg

Fig. 6 shows the effects of d-μg and s-μg on $[Ca^{2+}]_i$ inMC3T3-E1 cells. As shown in Fig. 6A-a to Fig. 6A-d, MC3T3-E1 cells exposed to d-μg showed increased fluorescence intensity (Fig. 6A-b *vs.* Fig. 6A-a), but the cells exposed to s-μg showed decreased fluorescence intensity compared to the cells at 1g (Fig. 6A-c *vs.* Fig. 6A-d). Quantitatively, μg increased the $[Ca^{2+}]_i$ level from 274 ± 17 nM at 1g to 448 ± 29 nM at d-μg($p < 0.01$, Fig. 6B-a left), but reduced it from 435 ± 19 nM at 1g to 235 ± 16 nM at s-μg ($p < 0.01$, Fig. 6B-a right), respectively. Therefore, d-μg increased $[Ca^{2+}]_i$ in MC3T3-E1 cells by 63% but s-μg reduced $[Ca^{2+}]_i$ in MC3T3-E1 cells by 46% (Fig. 6C-a).

When pretreated with Gd, the change of $[Ca^{2+}]_i$ in MC3T3-E1 cells due to d-μg or s-μg was different. In the presence of Gd, the cells appeared to diminish their response to d-μg as shown by both the fluorescence images (Fig. 6A-e *vs.* Fig. 6A-f) and the quantified fluorescence intensity of $[Ca^{2+}]_i$ (258 ± 22 nM *vs.* 249 ± 17 nM for 1g*vs.*d-μg, NS, Fig. 6B-b/left), but the cells still responded to s-μgby reducing the $[Ca^{2+}]_i$ level from 388 ± 23 nM at 1g to 320 ± 37 nM at s-μg (1g *vs.* s-μg, $p < 0.01$, Fig. 6B-b right). Therefore, the ratio of $[Ca^{2+}]_i$change at μg compared to that at 1g was significantly different between the cells exposed to d-μg and s-μg in the presence of Gd (-3% *vs.* -18%, $p < 0.01$, Fig. 6C-b).

However, in the presence of CytoB, the cells still appeared to respond to d-μg by increasing the $[Ca^{2+}]_i$ level from 160 ± 11nM at 1g to 284 ± 20 nM at d-μg (Fig. 6i *vs.* Fig. 6j, Fig. 6B-c left, $p < 0.01$). Furthermore, in the presence of CytoB, the cells appeared to not respond to s-μg(Fig. 6k *vs.* Fig. 6l; 6B-c right). Therefore, in the presence of CytoB, d-μg caused $[Ca^{2+}]_i$ in the cells to increase by 77%, and s-μg caused $[Ca^{2+}]_i$ to increase by 7%, as compared to at 1g, respectively ($p < 0.01$, Fig. 6C-c).
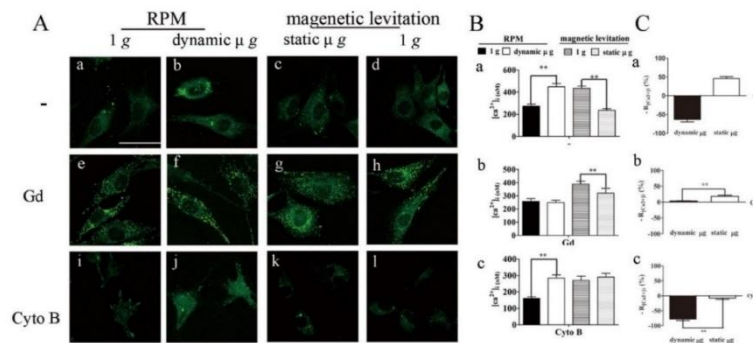
Figure 6: The calcium concentration changes in MC3T3-E1 cells exposed to either dynamic or static stimulated μg.

A) Images were captured with a laser confocal scanning microscope. Cells without drugs

(a, b, c, d) or treated with gadolinium chloride (Gd, 100 nM, e, f, g, h) and cytochalasin B (CytoB, 5 µM, i, j, k, l) were loaded with Fluo-3/AM and cultured under 1g, dynamic or static stimulated µg(dynamic µg and static µg)conditions for 3 h. Scale bar represents 50 µm. B) The summary data of $[Ca^{2+}]_i$ in MC3T3-E1 cells under the above-described conditions are shown. For each group, single cell (n = 30) was randomly selected and the fluorescence intensity per cell was digitized using Leica Image Manager Software. $[Ca^{2+}]_i$ was calibrated according to the equation: $[Ca^{2+}] = K_d \times [F_{(t)} - F_{min}]/[F_{max} - F_{(t)}]$. C) Histogram shows the ratio of $[Ca^{2+}]_i$ change in MC3T3-E1 cells exposed to dynamic and static µg. Histogram is shown as the mean $\pm$ SD. Statistically significant differences are indicated as $^*p< 0.05$, $^{**}p< 0.01$.

4 Discussion

In this study, we found that both d-µg and s-µg were able to alter CSK structure and calcium channel function of the cultured MC3T3-E1 cells in general, which are consistent with the previously published results. More importantly, we found that the cells responded to d-µg and s-µg differently in terms of the magnitude of morphological changes (cell shape and spreading area), assembly of microfilaments and microtubules as well as Ca^{2+}/CaM/CaMK signaling. For cell morphology and CSK structure, we found that d-µg was less potent than s-µg to induce cell rounding and protruding as well as CSK disruption. For Ca^{2+}/CaM/CaMK signaling, we found that d-µg and s-µg had opposite effect on Ca^{2+} influx, while d-µg was more potent than s-µg to inhibit CaM expression and CaMK activity.

Generally speaking, the cell's CSK and stretch-activated ion channels are considered the two primary components that are responsive to changing gravity because they are known to transform mechanical stress to chemical signal [Ingber (1999), Goldermann and Hanke (2001)]. In agreement with this notion, therefore, the overall effects of microgravity (both d-µg and s-µg) on the MC3TC-E1 cells can be attributed to changes in the CSK structure and Ca^{2+} signaling in response to change (decrease/loss in this case) of gravity force on the cells, as reported before [Hughes-Fulford (2003); Glade, Beaugnon and Tabony (2006), Heng anf Koh(2010), Glade and Tabony (2005)].

On the other hand, our results indicate that the differential responses of the MC3T3-E1 cells to d-µg and s-µg may be due to differential sensitivity of the CSK and the Ca^{2+} channels to specific way of gravity force reduction/elimination. For example, it is well known that CaM can bind to microfilaments and microtubules to regulate CSK organization [Xiang, Qi and Dai et al. (2010);Sullivan, Burnham and Torok et al. (2000), Wanget al. (2010)]. It is also known that CaMKis a serine/threonine-specific protein kinase that can be activated via Ca^{2+}-induced autophosphorylation and thus involved in regulation of microtubules [Lemieuxet al. (2012)] and microfilaments of the CSK [Khan, Conte and Carter et al. (2016)]. We show in our study that inhibition of CaM and CaMK indeed led to disruption of microfilaments and microtubules in cells, confirming the role of CaM and CaMK to mediate CSK assemblies.

Interestingly, when CaM was inhibited the differential responses of MC3T3-E1 cells to d-µg and s-µg in terms of cell morphology and CSK structures remained almost

unchanged. By contrast, CaMK inhibition diminished all those differential responses. When the calcium channels were inhibited, the responses of the cells to d-μg including cell morphology, CSK organization and $[Ca^{2+}]_I$ signaling were all diminished, but the responses due to s-μg were little affected. Moreover, disruption of microfilaments diminished the effect on Ca^{2+} signaling due to s-μg, but not that due to d-μg.

Considering all the above phenomena associated with changes of CSK and Ca^{2+} signaling due to d-μg and s-μg in the absence/presence of CSK and calcium channel manipulators such as W-7, KN-93, Gd and Cyto B, it is probably reasonable to assume that the stretch-activated calcium channels are only responsive to d-μg because the calcium channel blocker (Gd) was able to abolish all the responses of the cells to d-μg, but not those due to s-μg. The CSK structures, although may be responsive to both d-μg and s-μg, are probably more sensitive to s-μg based on the following arguments. First, when the calcium channels were intact, manipulation of the CSK organization by inhibiting CaM increased the difference of effect on the MC3T3-E1 cells induced by d-μg and s-μg, in particular the cell spreading and microfilament but not microtubule disruption. Since the d-μg effect was not changed in this case, s-μg effect should be largely responsible for the increased difference of effect between d-μg and s-μg in the event of CaM modulated changes in CSK organization, suggesting that CSK was sensitive to s-μg. Second, when the CSK structure was altered by inhibiting CaMK, the differences of effect between d-μg and s-μg including cell spreading, microfilaments and microtubules organization were diminished. Again, the d-μg effect was not changed in this case, the diminishing of the differences of effects between d-μg and s-μg should be mainly due to changes induced by s-μg, suggesting that, even if Ca^{2+} was involved the CaMK-associated CSK manipulation, the CSK structure was mainly responsible for the effect of s-μg. Finally, it should be also noted that Ca^{2+} may flow into cells through stretch-activated channels and result in the d-μg-induced disruptions of microfilaments and microtubules, but s-μg-induced CSK disorganization mediates the following $[Ca^{2+}]_i$ change.

The mechanism responsible for the differential sensitivity of CSK structure and calcium channel to d-μg and s-μg most likely lie in the fundamental difference of force acting on the cells as depicted in Fig. 7. When microgravity is stimulated on ground with RPM, d-μg was produced on objects such as cells situated inside the RPM by continuously moving the gravity vector in three dimensions in a random manner, which is called gravity-vector averaging [Grosse*et al.* (2012)]. During the rotation of organisms, the gravity still exists, but its direction constantly changes. In such movement, the cells are rotated and massaged by the gravity force, and the cytoplasm and large organelle in the cells, such as the nucleus, endoplasmic reticulum, and mitochondria, may change their positions and thus result in tension alteration inside the cells and even in cell membranes which may activate stretch sensitive channels (Fig.7A). In comparison, when microgravity is stimulated on ground with magnetic levitation, s-μg was generated on diamagnetic objects such as cells with a high gradient magnetic field [Beaugnon and Tournier (1991)]. Under s-μg condition, the direction of gravity does not change, but cells will be elevated steadily to a relaxed state by the magnetic force as compared to the more strained state under normal gravity (Fig. 7B). Thus, the cells will stay in a static environment, where the shearing stresses due to relative movement between cell and medium or intracellular components may be minimal so that the calcium channels may not be activated. The intracellular

tension may also be minimal in such relaxed state because the strong supporting force from the CSK structure (equiv. to great intracellular tension) for maintaining cell shape may become unnecessary, so that the microfilaments, microtubules, the nuclear CSK may all reorganize easily to adapt to new force conditions.
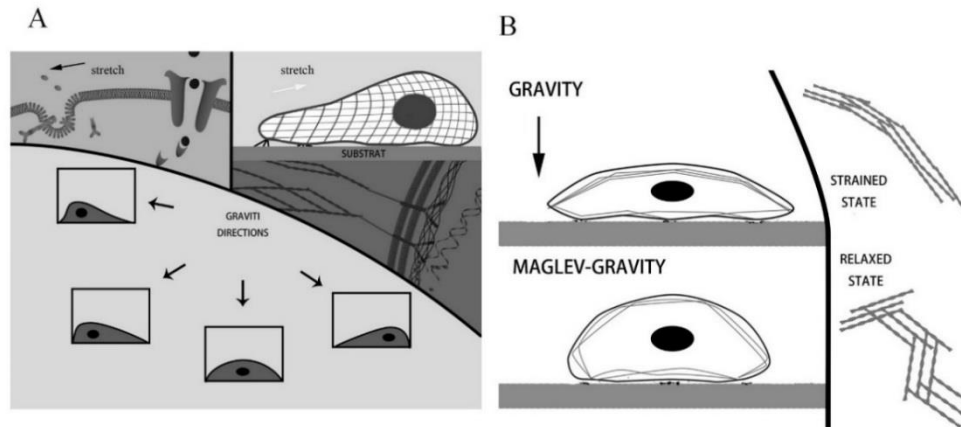
Figure 7: Different responses of osteoblasts to dynamic and static μg.

A) Under d-μg, the gravity still exists, but its direction constantly changes. As soft matters the cells are rotated and massaged by the gravity, and the cytoplasm and large organelles in the cells may change their locations resulting in the tension alterations inside the cells and even in cell membranes which may activate stretch sensitive channels. B) Under s-μg, the direction of gravity does not change, but the cells will change to a more relaxed state compared to those under normal gravity. The supporting system such as microfilament and microtubule in cells may reorganize their structure and distribution to adapt new force conditions (Fig. 7B).

Of course, the above mechanism is hypothetical at its best, and remains to be tested in future study. Nevertheless, together with the experimental results as described in this paper, it emphasizes the need to consider the limitations associated with specific ground-based method for simulation of microgravity. At least, when RPM is used, it should be known that the randomization of rotation requires time to statistically nullify gravity in all directions. Therefore only processes experiencing a certain time lag phase can be measured. It should also be noticed that the effects induced by d-μg with RMP may depend on the fashion of continuous changes of stress distribution determined by the rotation speed and direction. When diamagnetic levitation is used, on the other hand, it is important to properly take into account of the effect of magnetic field on biological processes in addition to force-induced responses in the system in order to explain the experimental results.

The observed phenomena that MC3T3-E1 cells responded differently to the microgravity condition stimulated by ground-based method of either RPM or magnetic levitation may have important implications in understanding the biological effects induced by various ground-based methods such as RPM and magnetic levitation, especially when they are used in biomedical research such as tissue engineering [Aleshchevaet al. (2013);Jaganathan et al. (2014);Durmus et al. (2015);Kopp et al. (2015)] and drug discovery [Ma et al. (2014)].

Perhaps most importantly, it should be kept in mind that any results obtained with microgravity stimulated on ground remain to be verified ultimately in real microgravity in space.

5   Conclusion

In summary, MC3T3-E1 cells display differential responses to the d-μg and s-μg stimulated with the RPM and diamagnetic levitation, respectively. Ca2+ flows into cells through stretch-activated channels and induces the CSK collapse in MC3T3-E1 cells under the d-μg, but calcium response induced by s-μg is regulated by changes of microfilaments. The inhibition of CaM and CaMKⅡ may also mediate the collapses of microfilaments and microtubules induced by stimulated microgravity using the RPM and diamagnetic levitation conditions.

Conflict of interest The authors declare that they have no conflict of interest.

Author Contributions Conception and design: P.S., L.H.D. and M.Z.L.; Acquisition of data: M.Z.L., Y.J., P.L.Y and X.Y.; Analysis and interpretation of data: M.Z.L., Y.J. and A.R.Q.; Drafting the manuscript: M.Z.L. and Y.J.; Revising the manuscript critically for important intellectual content: L.H.D.

References

Arfat, Y.;Xiao, W. Z.; Iftikhar, S.; Zhao, F.; Li, D. J.; Sun, Y. L.; Zhang, G.; Shang, P.; Qian, A. R.(2014): Physiological Effects of Microgravity on Bone Cells. *Calcified Tissue International,*vol. 94, pp. 569-579.

Aleshcheva, G.; Sahana, J.; Ma, X.; Hauslage, J.; Hemmersbach, R.; Egli, M.; Infanger, M.; Bauer, J.; Grimm, D.(2013): Changes in Morphology, Gene Expression and Protein Content in Chondrocytes Cultured on a Random Positioning Machine. *PLoS ONE,*vol. 8, pp. e79057.

Bauer, J.; Abou-El-Ardat, K; Baatout, S; Ma, X.; Infanger, M; Hemmersbach, R.; Grimm, D. (2012): Gravity-sensitive signaling drives 3-dimensional formation of multicellular thyroid cancer spheroids. *The FASEB Journal,*vol. 26, pp. 5124-5140.

Beaugnon, E.; Tournier, R. (1991): Levitation of organic materials. *Nature,*vol. 349: pp. 470-470.

Berry, M.V.; Geim, A. K. (1997): Of flying frogs and levitrons. *European Journal of*

*Physics,*vol. 18: pp. 307.

Borst, A. G.; van Loon, J. J. W. A.(2008): Technology and Developments for the Random Positioning Machine, RPM. *Microgravity Science and Technology,*vol. 21, pp. 287.

Durmus, N. G.; Tekin, H. C.; Guven, S.; Sridhar, K.; Arslan Yildiz, A.; Calibasi, G.; Ghiran, I.; Davis, R. W.; Steinmetz, L. M.; Demirci, U.(2015): Magnetic levitation of single cells. *Proceedings of the National Academy of Sciences of the United States of America,*vol. 112, pp. E3661-E3668.

Fuseler, J. W.; Millette, C. F.; Davis, J. M.; Carver, W. (2007): Fractal and image analysis of morphological changes in the actin cytoskeleton of neonatal cardiac fibroblasts in response to mechanical stretch. *Microscopy and microanalysis,*vol. 13: pp. 133-143.

Gillespie, P.G.; Walker, R. G.(2001): Molecular basis of mechanosensory transduction.*Nature,*vol. 413 pp. 194-202.

Glade, N.; Tabony, J. (2005): Brief exposure to high magnetic fields determines microtubule self-organisation by reaction-diffusion processes. *Biophysical Chemistry,*vol. 115, pp. 29-35.

Glade, N.; Beaugnon, E.; Tabony, J.(2006): Ground-based methods reproduce space-flight experiments and show that weak vibrations trigger microtubule self-organisation. *Biophysical Chemistry,*vol. 121, pp. 1-6.

Grosse, J.; Wehland, M.; Pietsch, J.; Schulz, J.; Saar, K.; Hübner, N.; Eilles, C.;

Goldermann, M.; Hanke, W. (2001): Ion channel are sensitive to gravity changes. *Microgravity Science and Technology,* vol. 13, pp. 35-38.

Hammer, B. E.; Kidder, L. S.; Williams, P. C.; Xu, W. W. (2009): Magnetic Levitation of MC3T3 Osteoblast Cells as a Ground-Based Simulation of Microgravity. *Microgravity science and technology,*vol. 21: pp. 311-318.

Heng, Y. W.; Koh, C. G. (2010): Actin cytoskeleton dynamics and the cell division cycle. *The International Journal of Biochemistry & Cell Biology,*vol. 42, pp. 1622-1633.

Hu, L. F.; Li, J. B.; Qian, A. R.; Wang, F.; Shang, P. (2015): Mineralization initiation of MC3T3-E1 preosteoblast is suppressed under simulated microgravity condition. *Cell Biology International,*vol. 39, pp. 364-372.

Hughes-Fulford, M. (2003): Function of the cytoskeleton in gravisensing during spaceflight. *Advances in space research,*vol. 32, pp. 1585-1593.

Ingber, D.(1999): How cells (might) sense microgravity. *TheFASEB Journal,*vol. 13 pp. S3-15.

Jaganathan H, Gage, J.; Leonard, F.; Srinivasan, S.; Souza, G. R.; Dave, B.; Godin, B. (2014): Three-Dimensional In Vitro Co-Culture Model of Breast Tumor using Magnetic Levitation. *Scientific Reports,*vol. 4 pp. 6468.

Kao, J. P.; Harootunian, A. T.; Tsien, R. Y. (1989): Photochemically generated cytosolic calcium pulses and their detection by fluo-3. *The Journal of biological chemistry,*vol. 264, pp. 8179-8184.

Khan, S.; Conte, I.; Carter, T.; Bayer, K. U.; Molloy Justin. E. (2016): Multiple CaMKII Binding Modes to the Actin Cytoskeleton Revealed by Single-Molecule Imaging. *Biophysical Journal,* vol. 111, pp. 395-408.

Kopp, S.; Slumstrup, L.; Corydon, T. J., ;Sahana, J.; Aleshcheva, G.; Islam, T.; Magnusson, N. E.; Wehland, M.; Bauer, J.; Infanger, M.; Grimm, D.(2016): Identifications of novel mechanisms in breast cancer cells involving duct-like multicellular spheroid formation after exposure to the Random Positioning Machine. *Scientific Reports,* vol. 6, pp. 26887.

Kopp, S.; Warnke, E.; Wehland, M.; Aleshcheva, G.; Magnusson, NE.; Hemmersbach, R.; Corydon, TJ.; Bauer, J; Infanger, M; Grimm, D.(2015): Mechanisms of three-dimensional growth of thyroid cells during long-term simulated microgravity. *Scientific Reports,* vol. 5, pp. 16691.

Lemieux, M.; Labrecque, S.; Tardif, C.; Labrie-Dion, É.; Lebel, É.; De Koninck, P. (2012): Translocation of CaMKII to dendritic microtubules supports the plasticity of local synapses. *The Journal of Cell Biology,* vol. 198, pp. 1055-1073.

Luo, M.; Yang, Z. Q.; Li, J. B.; Xu, H. Y.; Li, S. S.; Zhang, W.; Qian, A. R.; Shang, P. (2013): Calcium influx through stretch-activated channels mediates microfilament reorganization in osteoblasts under simulated weightlessness. *Advances in Space Research,* vol. 51, pp. 2058-2068.

Ma, X.;Pietsch, J.; Wehland, M; Schulz, H; Saar, K; Hübner, N; Bauer, J; Braun, M; Schwarzwälder, A; Segerer, J; Birlem, M; Horn, A; Hemmersbach, R.; Waßer, K.; Grosse, J.; Infanger, M.; Grimm, D.(2014): Differential gene expression profile and altered cytokine secretion of thyroid cancer cells in space. *The FASEB Journal,* vol. 28, pp. 813-835.

Moes, M. J, A.; Gielen, J. C.; Bleichrodt, B. J.; van Loon, J. J. W. A.; Christianen, P. C. M.; Boonstra, J. (2011): Simulation of Microgravity by Magnetic Levitation and Random Positioning: Effect on Human A431 Cell Morphology. *Microgravity Science and Technology,* vol. 23, pp. 249-261.

Pani, G.;Samari, N.; Quintens, R.; de Saint-Georges, L.; Meloni, M.; Baatout, S.; Van Oostveldt, P.; Benotmane, M. A.(2013): Morphological and Physiological Changes in Mature In Vitro Neuronal Networks towards Exposure to Short-, Middle- or Long-Term Simulated Microgravity. *PLoS ONE,* vol. 8, pp. e73857.

Qian, A.; Yin, D. C.; Yang, P. F.; Jia, B.; Zhang, W.; Shang, P.(2009): Development of a Ground-Based Simulated Experimental Platform for Gravitational Biology. *IEEE Transactions on Applied Superconductivity,* vol. 19, pp. 42-46.

Sambandam, Y.; Baird, K. L.; Stroebel, M.; Kowal, E.; Balasubramanian, S.; Reddy, S. V.(2016): Microgravity Induction of TRAIL Expression in Preosteoclast Cells Enhances Osteoclast Differentiation. *Scientific Reports,* vol. 6, pp. 25143.

Sanabria, H.; Swulius, M. T.; Kolodziej, S. J.; Liu, J.; Waxham, M. N. (2009): βCaMKII regulates actin assembly and structure. *The Journal of biological chemistry,* vol. 284, pp. 9770-9780.

Souza, G. R.; Molina, J. R.; Raphael, R. M.; Ozawa, M. G,; Stark, D. J.; Levin, C. S.; Bronk, L. F,; Ananta, J. S.; Mandelin, J.; Georgescu, M. M.; Bankson, J. A.;

Gelovani, J. G.; Killian, T. C.; Arap, W.; Pasqualini, R. (2010): Three-dimensional Tissue Culture Based on Magnetic Cell Levitation. *Nature nanotechnology,* vol. 5, pp. 291-296.

Sullivan, R.; Burnham, M.; Torok, K; Koffer, A. (2000): Calmodulin regulates the disassembly of cortical F-actin in mast cells but is not required for secretion. *Cell calcium* vol. 28, pp. 33-46.

Sun, J.;Liu, X.; Tong, J.; Sun, J.; Xu, H.; Shi, L,; Zhang, J. (2014): Fluid shear stress induces calcium transients in osteoblasts through depolarization of osteoblastic membrane. *Journal of biomechanics,* vol. 47, pp. 3903-3908.

Ulbrich, C.;Wehland, M.; Pietsch, J; Aleshcheva, G.; Wise, P; van Loon, J; Magnusson, N.; Infanger, M.; Grosse, J.; Eilles, C.; Sundaresan, A.; Grimm, D. (2014): The Impact of Simulated and Real Microgravity on Bone Cells and Mesenchymal Stem Cells. *BioMed Research International*, pp. 928507.

Van Loon, J.J.W.A. (2007): Some history and use of the random positioning machine, RPM, in gravity related research. *Advances in Space Research,* vol. 39, pp. 1161-1165.

Valles Jr, J. M.; Maris, H. J.; Seidel, G. M.; Tang, J.; Yao, W.(2005): Magnetic levitation-based Martian and Lunar gravity simulator. *Advances in Space Research,* vol. 36, pp. 114-118.

Wang, Q.; Symes, A. J; Kane, C. A.; Freeman, A.; Nariculam, J.; Munson, P.; Thrasivoulou, C.; Masters, J. R.; Ahmed, A. (2010): A novel role for Wnt/Ca2+ signaling in actin cytoskeleton remodeling and cell motility in prostate cancer. *PLoS One,* vol. 5, pp. e10456.

Wang, Y.; Chen, Z. H.; Yin, C.; Ma, J. H,; Li, D. J.; Zhao, F.; Sun, Y. L.; Hu, L. F.; Shang, P.; Qian, A. R.(2015): GeneChip Expression Profiling Reveals the Alterations of Energy Metabolism Related Genes in Osteocytes under Large Gradient High Magnetic Fields. *PLoS ONE,* vol. 10, pp. e0116359.

Wuest, S. L.; Richard, S.; Kopp, S.; Grimm, D.; Egli, M.(2015): Simulated Microgravity: Critical Review on the Use of Random Positioning Machines for Mammalian Cell Culture. *BioMed Research International,* vol. 2015: pp. 971474.

Xiang, L.; Qi, F.; Dai, D.; Li, C.; Jiang, Y.(2010): Simulated microgravity affects growth of Escherichia coli and recombinant beta-D-glucuronidase production. *Applied biochemistry and biotechnology,* vol. 162, pp. 654-661.

Zhang, S.; Zheng, D.; Wu, Y.; Lin, W.; Chen, Z.; Meng, L.; Liu, J.; Zhou, Y. (2016): Simulated Microgravity Using a Rotary Culture System Compromises the In Vitro Development of Mouse Preantral Follicles. *PLoS ONE,* vol. 11, pp. e0151062.

Zhang, C.; Zhou, L.; Zhang, F.; Lü, D.; Li, N.; Zheng, L.; Xu, Y.; Li, Z.; Sun, S.; Long, M. (2017): Mechanical remodeling of normally sized mammalian cells under a gravity vector. *The FASEB Journal,* vol. 31, pp. 802-813.

Zhang, J.; Li, J. B.; Xu, H. Y,; Yang, P. F.; Xie, L.; Qian, A. R.; Zhao, Y.; Shang, P.(2015): Responds of Bone Cells to Microgravity: Ground-Based Research. *Microgravity Science and Technology*, vol. 27, pp. 455-464